MTHFD2 Ablation in T Cells Protects against Heart Transplant Rejection by Perturbing IRF4/PD-1 Pathway through the Metabolic-epigenetic NexusRunning Title: MTHFD2 ablation protects heart transplant rejection

Yuan Li, Zhang Chen, Jikai Cui, Jizhang Yu, Yuqing Niu, Shuan Ran, Song Wang, Weicong Ye, Heng Xu, Xi Zhang, Jie Wu, Jiahong Xia

PII: S1053-2498(23)01940-X

DOI: https://doi.org/10.1016/j.healun.2023.07.009

Reference: HEALUN7962

To appear in: *Journal of Heart and Lung Transplantation*

Please cite this article as: Yuan Li, Zhang Chen, Jikai Cui, Jizhang Yu, Yuqing Niu, Shuan Ran, Song Wang, Weicong Ye, Heng Xu, Xi Zhang, Jie Wu and Jiahong Xia, MTHFD2 Ablation in T Cells Protects against Heart Transplant Rejection by Perturbing IRF4/PD-1 Pathway through the Metabolic-epigenetic NexusRunning Title: MTHFD2 ablation protects heart transplant rejection, *Journal of Heart and Lung Transplantation,* (2023) doi:https://doi.org/10.1016/j.healun.2023.07.009

MTHFD2 Ablation in T Cells Protects against Heart Transplant Rejection by Perturbing IRF4/PD-1 Pathway through the Metabolic-epigenetic Nexus

Yuan Li[1,2#], Zhang Chen[1,2#], Jikai Cui[1,2#], Jizhang Yu[1,2], Yuqing Niu[1,2], Shuan Ran[1,2], Song Wang[1,2], Weicong Ye[1], Heng Xu[1,2], Xi Zhang[1,2*], Jie Wu[1,2,3*], Jiahong Xia[1,2,3*]

[1] Department of Cardiovascular Surgery, Union Hospital, Tongji Medical College, Huazhong University of Science and Technology, Wuhan 430022, China; [2]Center for Translational Medicine, Union Hospital, Tongji Medical College, Huazhong University of Science and Technology, Wuhan, China.[3]Key Laboratory of Organ Transplantation, Ministry of Education, NHC Key Laboratory of Organ Transplantation, Key Laboratory of Organ Transplantation, Chinese Academy of Medical Sciences, Wuhan, China

# These authors contributed equally to this work.

*Correspondence: Jiahong Xia, E-mail: jiahong.xia@mail.hust.edu.cn; Jie Wu, E-mail: wujie426@hust.edu.cn; Xi Zhang, E-mail: zhangxi798@sina.com

Running Title: MTHFD2 ablation protects heart transplant rejection

Word Count: Manuscript: 2999, Abstract: 237, **Figures:** 8

Non-standard Abbreviations:

1C, One-carbon;

GSEA, gene set enrichment analysis;

IRF4, interferon regulatory factor 4;

MLR, mixed lymphocyte reaction;

MTHFD2, methylenetetrahydrofolate dehydrogenase 2;

PD-1, programmed death-1;

SAM, s-adenosyl methionine;

GITs, graft-infiltrating T cells.

Abstract

Background: One-carbon metabolism supports the activation, proliferation, and function of multiple immune cells. However, researchers have not clearly determined whether and how one-carbon metabolic enzymes contribute to heart transplant rejection.

Methods: We investigated the dynamic metabolic adaptation in grafts during heart transplant rejection by conducting transcriptomics, metabolomics and single-cell RNA sequencing studies of cardiac tissue from human and mouse heart transplant recipients. We also assessed the expression of the one-carbon metabolic enzyme MTHFD2 in cardiac grafts by immunofluorescence and flow cytometry assays. Then we constructed a murine heart transplant model with T cell-specific *Mthfd2* knockout mice, analyzed T cells function by flow cytometry assays and enzyme-linked immunospot assays, and studied the mechanism by Cleavage Under Targets and Tagmentation assays. Finally, we studied the effect of a pharmacological inhibitor of MTHFD2 in humanized skin transplant model.

Results: We revealed that the one-carbon metabolism enzyme MTHFD2 was a hallmark of alloreactive T cells and was linked to T cell proliferation and function after exposure to alloantigen. And, *Mthfd2* ablation prevented murine heart transplant rejection. Mechanistically, we found *Mthfd2* ablation affected the IRF4/PD-1 pathway through a metabolic-epigenetic mechanism involving H3K4me3. Furthermore, we found that inhibiting MTHFD2 attenuated human allograft rejection in a humanized skin transplant model.

Conclusions: These data show that the one-carbon metabolic enzyme MTHFD2 serves as a metabolic checkpoint of alloreactive T cells and suggest that it may be a potential therapeutic target for heart transplant rejection.

Keywords: One-carbon metabolism, MTHFD2, IRF4, Heart transplant rejection, T cells.

Introduction

Cellular metabolism involves complex sequences of controlled biochemical reactions, which allow organisms to grow and respond to environmental changes(1). The stimulation of T cells induces metabolic reprogramming to cultivate effector T cells and long-lived memory cells, which are essential for T-cell function and fate(2). Folate metabolism, which is also known as one-carbon (1C) metabolism, is a universal metabolic process that activates and transfers 1C units for biosynthetic processes and cellular functions(3-5). 1C metabolism is closely related to T cell receptor stimulation and is essential for T-cell expansion(6, 7). In addition, it generates the universal methyl donor S-adenosyl methionine (SAM) for protein and DNA methylation to modify T-cell function(7, 8). T cells are critical cells promoting heart transplant rejection(9). For instance, $CD4^+$ T helper cells promote the differentiation of $CD8^+$ T cells into alloreactive effectors and provide help to B cells, enabling them to generate a humoral response; these immune responses result in graft injury and rejection(10). However, the role of 1C metabolism in T-cell-mediated rejection is unclear.

Methylenetetrahydrofolate dehydrogenase 2 (MTHFD2) is one of the main enzymes involved in 1C metabolism and is also known as NAD-dependent mitochondrial methylenetetrahydrofolate dehydrogenase-cyclohydrolase(11-13). MTHFD2 is upregulated in various cancers and developing embryos but remains at low to undetectable levels in most differentiated normal adult tissues(14). In addition, high MTHFD2 expression is associated with poor outcomes in many diseases, such as autoimmune disease (15). Recent studies have shown that MTHFD2 expression is increased in activated T cells *in vivo* and *in vitro* (12, 16). Importantly, MTHFD2

inhibition or genetic deficiency reduces the severity of T-cell-mediated diseases, such as experimental autoimmune encephalomyelitis, inflammatory bowel disease (3, 17). Nevertheless, researchers have not determined whether MTHFD2 inhibition prevents heart transplant rejection.

In this study, we performed RNA sequencing and single-cell RNA-seq analysis. Then, we found that MTHFD2 was upregulated in allografts. Additionally, T-cell-specific *Mthfd2* deficiency inhibited heart transplant rejection. Mechanistically, *Mthfd2* ablation affected the IRF4/PD-1 pathway through a metabolic-epigenetic mechanism involving H3K4me3. Moreover, MTHFD2 inhibition prevented skin transplant rejection in humanized mice. These data show that MTHFD2 serves as a metabolic checkpoint in alloreactive T cells and highlight the potential of MTHFD2 as a target for heart transplant rejection immunotherapy.

Materials and Methods

Detailed descriptions of experimental materials and methods are available in the Supplementary Materials and Methods.

Murine heterotopic heart transplantation

Murine heterotopic heart transplantation was performed as previously described(18, 19). The details are provided in the Supplementary Material and Methods.

Humanized skin transplant model

All human samples were collected with permission from the double eyelids' operation patients. Humanized skin transplantation was performed as previously described(20, 21).The details are provided in the Supplementary Material and Methods.

Mouse study and Human sample approval

Animal protocols were reviewed and approved by the Institutional Animal Care and Use Committee of Huazhong University of Science and Technology and complied with the National Institutes of Health Guidelines for the Care and Use of Laboratory Animals. Human sample studies were approved by the Research Ethics Committee of Union Hospital, Tongji Medical College, Huazhong University of Science and Technology (Approval No. XWK-YZMY-63) and were performed in accordance with the principles of the 1975 Declaration of Helsinki. Specimen were not obtained from prisoners or deceased individuals.

Statistical analysis

Data are presented as the means (SD) or interquartile range. The p values were analyzed with GraphPad Prism Software (version 9.0). The statistical analyses are listed in revised Supplementary material and the figure legends. Statistical significance was set to $p < 0.05$.

Results

1C metabolism is significantly active in graft-infiltrating T cells (GITs) during heart transplant rejection

We conducted transcriptomic and metabolomic analyses to investigate the dynamic metabolic adaptation in grafts during heart transplant rejection. A total of 1341 genes were differentially expressed in the allografts compared with the isografts (Figure 1B). Then, we performed gene set enrichment analysis (GSEA) of the differentially expressed genes (DEGs) and identified representative pathways associated with allograft rejection, T-cell function and metabolism, including IL2_PATHWAY, ALLOGRAFT_REJECTION, TCR_PATHWAY, and FOLATE_METABOLISM (Figure 1C-D, Supplementary Table 2). We also analyzed endomyocardial biopsies from patients with or without rejection after heart transplant in the clinic (data from GSE150059) (22). GSEA revealed that the main biological processes of the signature included not only ALLOGRAFT_REJECTION,

MODULATORS_OF_TCR_SIGNALING _AND_T_CELL_ACTIVATION but also FOLATE_METABOLISM (1C metabolism) (Supplementary Figure 1A-B, Figure 1E, Supplementary Table 2). Moreover, we performed a metabolomics analysis of cardiac grafts and found that the levels of some nucleotides related to 1C metabolism were significantly different between isografts and allografts (Figure 1F). We performed scRNA-Seq of $CD45^+$ cells from BALB/c transplanted and native untransplanted hearts to explore the differences in 1C metabolism in various immune cells present in the hearts (Figure 1G) (22, 23). Based on the typical marker genes, 4 clusters (T cells, B cells, macrophages, and neutrophils) were identified (Supplementary Figure 2, Figure 1G). The enrichment score for 1C metabolism in T cells present in the heart with heart transplant rejection was significantly increased, but the enrichment score for neutrophils was reduced (Figure 1H). Together, these data indicate that 1C metabolism is significantly more active in GITs during heart transplant rejection.

The 1C metabolic enzyme MTHFD2 is expressed at high levels in GITs during heart transplant rejection

We screened potential targets related to 1C metabolism in graft-infiltrating T cells during heart transplant rejection by analyzing the expression of genes encoding 1C metabolic enzymes in allografts and isografts using RNA-seq and found that *Mthfd2* was one of the most highly induced genes in allografts (Figure 2A). Similar upregulation of *MTHFD2* in human endomyocardial biopsies with heart transplant rejection was observed (Figure 2B). We analyzed the scRNA-seq data to determine *Mthfd2* expression in different types of immune cells in cardiac allografts during heart transplant rejection, and the results shown in Figure 1 indicated that *Mthfd2* was predominantly expressed in GITs (Figure 2C). Next, we collected the mouse cardiac allograft for the immunofluorescence staining and found that MTHFD2 was mainly presented in GITs (Figure 2D). We isolated graft-infiltrating cells for flow cytometry

assays to quantitatively analyze MTHFD2 levels in graft-infiltrating T-cells (Supplementary Figure 3). MTHFD2 expression was significantly increased in both graft-infiltrating $CD4^+$ and $CD8^+$ T cells of allografts compared with isografts (Figure 2E- F, n=5). Thus, the 1C metabolic enzyme MTHFD2 is expressed at high levels in GITs during heart transplant rejection.

T-cell-specific *Mthfd2* deficiency prevents heart transplant rejection in mice

We generated T-cell-specific *Mthfd2* knockout mice (*Mthfd2*$^{fl/fl}$*Cd4-Cre*$^+$) and established a fully MHC-mismatched heart transplantation model to evaluate the role of MTHFD2 in T-cell-mediated heart transplant rejection. The survival of cardiac allografts in the *Mthfd2*$^{fl/fl}$*Cd4-Cre*$^+$ mice was significantly prolonged compared with that in the *Mthfd2*$^{fl/fl}$ mice (Figure 3A, n=7). Meanwhile, the histopathology analysis of cardiac allografts showed a diffuse lymphocyte infiltrate accompanied by multifocal myocyte damage in *Mthfd2*$^{fl/fl}$ mice, while only limited lymphocyte infiltration was observed in *Mthfd2*$^{fl/fl}$*Cd4-Cre*$^+$ mice (Figure 3B, n=5). Using a flow cytometry assay, we found that T-cell-specific *Mthfd2* knockout decreased $CD4^+$ and $CD8^+$ T-cell proportion and number in the spleen during acute rejection (Figure 3C, n=5). The percentages of IL-17- and IFN-γ-producing $CD4^+$ T-cells and IFN-γ-producing $CD8^+$ effector T cells were decreased in *Mthfd2* knockout mice (Figure 3D-E, n=5), while the percentage of regulatory T cells was increased in the recipient spleen (Figure 3F). In addition, T-cell-specific *Mthfd2* knockout led to a decrease in splenic IFN-γ-producing alloreactive cells, as detected using an enzyme-linked immunospot (ELISpot) assay (Figure 3G, n=5). Taken together, these data revealed that T-cell-specific *Mthfd2* knockout impaired the function of alloreactive T cells and prevented heart transplant rejection in mice.

***Mthfd2* deficiency promotes the long-term survival of mouse models in chronic heart transplant rejection**

We investigated the effects of T-cell-specific *Mthfd2* deletion on chronic heart transplant rejection. *Mthfd2*$^{fl/fl}$ or *Mthfd2*$^{fl/fl}$*Cd4-Cre*$^{+}$ mice were transplanted with BALB/c hearts, and then recipients were treated with 250 μg of CTLA-4-Ig on day 2 posttransplant (Figure 4A, n=6). The survival of cardiac allografts was significantly increased in *Mthfd2*$^{fl/fl}$*Cd4-Cre*$^{+}$ mice (Figure 4B). Histologically, cardiac allografts from *Mthfd2*$^{fl/fl}$ recipient mice were characterized by much more serious perivascular cellular infiltration and vascular occultation at day 28 post transplantation than those from *Mthfd2*$^{fl/fl}$*Cd4-Cre*$^{+}$ mice (Figure 4C-D, n=5). We also observed more collagen deposits in cardiac allografts from *Mthfd2*$^{fl/fl}$ recipient mice than in those from *Mthfd2*$^{fl/fl}$*Cd4-Cre*$^{+}$ mice (Figure 4C-D). Based on these results, *Mthfd2* ablation in T cells inhibits chronic heart transplant rejection in mice.

MTHFD2 is required for the function and IRF4 expression of alloreactive T cells in an H3K4me3-dependent manner

We generated TEa$^{Mthfd2\ KO}$ (TEa ×*Mthfd2*$^{fl/fl}$*Cd4-Cre*+, KO) mice and TEa^{WT} (TEa ×*Mthfd2*$^{fl/fl}$, WT) mice to analyze the effects of *Mthfd2* deficiency on alloreactive T-cell function and the underlying mechanisms. CD4^{+} TEa cells were isolated from spleens using magnetic-activated cell sorting, labelled with CFSE, and then cocultured with mitomycin C-treated antigen-presenting cells (APCs) from BALB/c × C57BL/6 F1 mice. After 72 h of coculture, we found that *Mthfd2* deficiency inhibited alloreactive T-cell proliferation (Figure 5A, n=5). Meanwhile, IFN-γ production was also decreased in TEa$^{Mthfd2\ KO}$ cells (Figure 5B). The results indicated that *Mthfd2* deletion impaired the function of alloreactive T cells. We performed an RNA-seq analysis of KO and WT TEa cells to study the mechanism of T-cell dysfunction after *Mthfd2* deletion. As shown in Figure 5C, 90 genes were downregulated and 153 genes were upregulated in KO cells compared with WT cells. The downregulated genes included genes encoding proinflammatory cytokines (IL2, IL22, IFN-g, and TNF), chemokines (CCL3 and CXCL13) and metabolism-related receptors (SLC4A1 and

SLC29a2) (Figure 5D). Moreover, the mRNA level of IRF4, which is an important transcription factor for T-cell function and fate(18), was significantly downregulated in *Mthfd2*-deficient TEa cells compared with WT TEa cells (Figure 5D). Consistent with the change in the *Irf4* mRNA level, we also found that IRF4 expression was decreased in *Mthfd2*-deficient TEa cells (Figure 5E, n=5). MTHFD2 is a 1C metabolism enzyme (24, 25) and is important for the production of SAM for protein and DNA methylation to modulate T-cell function (5, 26). The supernatant of the medium was collected for ELISA assay and found that SAM production was decreased in *Mthfd2*-deficient TEa cells compared with WT TEa cells (Figure 5F, n=5). As SAM is essential for histone methylation(27, 28), we detected the methylation level of representative histones in TEa cells. Although no differences in H3K36me3 and H3K27me3 levels were observed, the level of H3K4me3 was markedly decreased in *Mthfd2*-deficient TEa cells (Figure 5G, n=5). We performed H3K4me3 CUT&Tag assays (29) in *Mthfd2*-deficient and WT TEa cells to study the chromatin profile of H3K4me3 modification and found that the enrichment of H3K4me3 at the *Irf4* gene was decreased in *Mthfd2*-deficient T cells (Figure 5H).

MTHFD2 is required to maintain the formate pool for purine synthesis (7). Formate plays an important role in the proliferation, viability, and activation of $CD4^+$ T cells(30, 31). Next, we analyzed the effects of exogenous formate on H3K4me3 and IRF4 expression in *Mthfd2*-deficient T cells. The reduction in both H3K4me3 levels and IRF4 expression in *Mthfd2*-deficient T cells was rescued by exogenous formate (Figure 5I-J, n=5). Moreover, the reduced IFN-γ production was also rescued upon formate treatment (Figure 5K). Overall, these data suggest that *Mthfd2* deletion inhibits proliferation, IFN-γ production and IRF4 expression in alloreactive T cells in an H3K4me3-dependent manner.

The protective effect of *Mthfd2* ablation on heart transplant rejection depends on the PD-1 pathway

IRF4 ablation promoted the expression of the inhibitory receptor PD-1 in a cell intrinsic manner and mediated impaired cellular metabolism(9, 32). In the absence of IRF4, the chromatin accessibility of *Pdcd1* is increased, which results in enhanced PD-1 expression and dysfunction(9). Subsequently, we further analyzed the RNA-seq data in Figure 5C to investigate the expression of immune checkpoint genes that promote T-cell exhaustion and dysfunction(32) and found that Pdcd1 (encoding PD-1) expression was significantly increased in *Mthfd2*-deficient TEa cells (Figure 6A). Also, we detected increased expression of PD-1 in *Mthfd2*-deficient TEa cells using an FCM assay (Figure 6B, n=5). We explored whether the protective effects of the T-cell-specific *Mthfd2* knockout on heart transplant rejection were associated with the PD-1 pathway by generating a mouse heart transplant rejection model (*Mthfd2*$^{fl/fl}$*Cd4-Cre*$^{+}$ mice as the recipient and BALB/c mice as the donor) and treated them with rat IgG or anti-PD-L1 mAb (Figure 6C, n=5). The survival of allografts was shortened, the lymphocyte infiltration and myocardial damage of allografts was increased with anti-PD-L1 treatment (Figure 6D-E). An analysis of the International Society for Heart and Lung Transplantation (ISHLT) grade of the allografts indicated that a higher score for anti-PD-L1-treated mice (Figure 6E). These data suggest that the protective effect of *Mthfd2* ablation on heart transplant rejection depends on the PD-1 pathway.

MTHFD2i administration attenuates human allograft rejection in humanized mice

We treated recipient mice of a humanized skin transplant with an MTHFD2 inhibitor (MTHFD2i; LY345899) to investigate the clinical translation of the effect of this inhibitor on heart transplant rejection. In this model, NSG mice were transplanted with human skin and then reconstituted with peripheral blood mononuclear cells (PBMCs) at 30 days after transplantation. The PBMC-reconstituted mice were treated with either vehicle or MTHFD2i (Figure 7A, n=10). The administration of MTHFD2i

obviously prolonged the survival of skin grafts (Figure 7B). The skin grafts were harvested on day 28 after PBMCs were reconstituted for HE and immunohistochemical staining. As shown in Figure 7C, lymphocyte infiltration in the skin graft was inhibited by MTHFD2i treatment. The expression of *CD3E* and *IRF4* mRNA was also reduced in the skin grafts from MTHFD2i-treated recipients (Figure 7D, n=5). Taken together, the humanized skin transplant model suggests that MTHFD2i attenuates allograft rejection and highlights the clinical translational potential of MTHFD2i for organ rejection following transplantation.

Discussion

The T-cell function requires appropriate metabolic reprogramming to meet the increased demands for energy, biosynthesis, and signaling molecules(33). 1C metabolism is central to several processes, including de novo purine synthesis, methyl donor generation(11, 34), which involved in the occurrence and prognosis of many diseases(34, 35). In our study, 1C metabolism was obviously activated in allografts, which was also verified by the metabolomic analysis. Furthermore, we proved that 1C metabolism was most significantly upregulated in GITs. These results suggest that 1C metabolism may play a critical role in alloreactive T cells. Activated T cells use complex metabolic pathways to generate the precursors required for macromolecular synthesis, energy and other prosurvival pathways (36, 37). Since many enzymes are indispensable for 1C metabolism(38), we screened the major enzymes of 1C metabolism in grafts and found that the *Mthfd2* gene was upregulated to the greatest extent during heart transplant rejection. Similar findings were obtained from endocardial biopsies in clinical. Moreover, our results revealed that the MTHFD2 mRNA and protein were mainly present in GITs. For further investigation, we found that *Mthfd2* deficiency prolonged cardiac allograft survival and inhibited the alloreactive T-cell response. These results suggest that MTHFD2 promotes T-cell-mediated rejection. Likewise, MTHFD2 regulates other diseases related to T cells. Ayaka et al. established that MTHFD2 inhibition or genetic deficiency ameliorated autoimmunity and hypersensitivity(17). Finally, we found that *Mthfd2* deficiency protected against not only acute cellular rejection but also cardiac allograft vasculopathy. Taken together, MTHFD2 and 1C metabolism are important in heart transplant rejection.

We employed a cell coculture assay to elucidate the mechanism underlying the effect of MTHFD2 on alloreactive T cells. *Mthfd2* ablation inhibited the proliferation and IFN-γ production of alloreactive T cells. Moreover, IRF4 expression was decreased in *Mthfd2* knockout alloreactive T cells. 1C metabolism regulates the

generation of the universal methyl donor SAM for protein and DNA methylation to modify T-cell function(27, 39). Our data showed that *Mthfd2* deficiency decreased the SAM concentration in T cells. Methionine contributes to gene transcription through SAM-dependent histone modifications(8, 40, 41). We assessed the effect of MTHFD2 on global H3 histone methylation in alloreactive T cells and found that H3K4me3 modifications were significantly affected by *Mthfd2* deficiency. We next performed the CUT&Tag assay to assess the H3K4me3 methylation patterns of the *Irf4* gene in alloreactive T cells. H3K4me3 marks were reduced across the TSS and gene body regions of the *Irf4* gene in *Mthfd2*-deficient alloreactive T cells, consistent with the reduced *Irf4* mRNA expression observed in *Mthfd2*-deficient alloreactive T cells. MTHFD2 activity contributes to maintain the intracellular formate pool(7). We performed rescue experiments by replenishing formate and confirmed that the effects of *Mthfd2* deficiency were weakened when formate was present. IRF4 is a key transcription factor that manipulates T-cell responses and represses PD-1, which is an inhibitory receptor expressed on activated T cells that dampens TCR /CD28 signaling by engaging with PD-L1 and associated with T-cell dysfunction (9, 42, 43). Through *in vitro* experiments, we found that PD-1 expression was increased in *Mthfd2*-deficient alloreactive T cells. Importantly, PD-1 blockade was capable of abrogating the protective effect of *Mthfd2* deficiency after heart transplantation. Finally, we proved that MTHFD2i also relieved skin transplant rejection in humanized mice. Taken together, our results revealed that MTHFD2 regulates the IRF4/PD-1 pathway through a metabolic-epigenetic mechanism involving H3K4me3 (Figure 8).

There are some limitations in our study: (1) Ischemia-reperfusion injury is believed to contribute to early allograft dysfunction(44, 45). The association of MTHFD2 with ischemic injury needs further investigation. (2) The immunosuppression regimen has never been used, and whether these agents affect 1C metabolism deserves to be explored. (3) As different nucleosides between isografts and allografts are not specific to the 1C pathway, further studies are required to

explore the role of other important pathways that involve these metabolites. (4) Whether AlloMap (46) genes, including *ITGA4*, *MARCH8* are regulated by MTHFD2 metabolism during heart transplant rejection is unclear and requires further study. (5) There were no donor-specific antibodies or biopsies/autopsies performed to correlate MTHFD2 expression with rejection in our study. (6) The effects of *Mthfd2* knockout on $CD8^+$ T-cell function in heart transplant rejection needs further study. (7) The gating strategy of $CD4^+$ and $CD8^+$ T cells in FCM assay never used T cell markers such as CD3. Nonetheless, our data reveal that MTHFD2 serves as a metabolic checkpoint in alloreactive T cells and highlight the potential of this enzyme as a target for heart transplant rejection immunotherapy.

Author Contributions

JW and JX conceived and designed the experiments; YL, XZ and ZC drafted the manuscript; YL, ZC, JY, JC, YN, SW and WY performed the experiments; RS and HX analyzed the data. All authors approved the final version of the manuscript.

Acknowledgments

We acknowledge the Medical Subcenter at HUST Analytical & Testing Center for its outstanding services. We thank Dr. Long Yu for technical guidance.

Funding

This study was supported by the National Natural Science Foundation of China (82071803, 82271811, 81730015, 82241217).

Conflict of interest

These authors declare that there is no conflict of interest in this work.

Data availability statement

All data are available from the corresponding author upon reasonable request.

References

1. Emambokus N, Granger A: Cell Metabolism Clinical and Translational Reports. Cell Metab 2015;22:2-3.

2. Madden MZ, Rathmell JC: The Complex Integration of T-cell Metabolism and Immunotherapy. Cancer Discov 2021;11:1636-43.

3. Ducker GS, Rabinowitz JD: One-Carbon Metabolism in Health and Disease. Cell metabolism 2017;25:27-42.

4. Morellato AE, Umansky C, Pontel LB: The toxic side of one-carbon metabolism and epigenetics. Redox Biology 2021;40:101850.

5. Ducker GS, Chen L, Morscher RJ, et al.: Reversal of Cytosolic One-Carbon Flux Compensates for Loss of the Mitochondrial Folate Pathway. Cell metabolism 2016;23:1140-53.

6. Tan H, Yang K, Li Y, et al.: Integrative Proteomics and Phosphoproteomics Profiling Reveals Dynamic Signaling Networks and Bioenergetics Pathways Underlying T Cell Activation. Immunity 2017;46:488-503.

7. Ma EH, Bantug G, Griss T, et al.: Serine Is an Essential Metabolite for Effector T Cell Expansion. Cell metabolism 2017;25:482.

8. Dai Z, Mentch SJ, Gao X, Nichenametla SN, Locasale JW: Methionine metabolism influences genomic architecture and gene expression through H3K4me3 peak width. Nature communications 2018;9:1955.

9. Wu J, Zhang H, Shi X, et al.: Ablation of Transcription Factor IRF4 Promotes Transplant Acceptance by Driving Allogenic CD4 T Cell Dysfunction. Immunity 2017;47.

10. Aliyari Serej Z, Ebrahimi Kalan A, Mehdipour A, Nozad Charoudeh H: Regulation and roles of CD26/DPPIV in hematopoiesis and diseases. Biomed Pharmacother 2017;91:88-94.

11. Gouirand V, Rosenblum MD: MTHFD2, metabolic mastermind of CD4(+) T cell destiny. Science immunology 2022;7:eabo6765.

12. Sugiura A, Andrejeva G, Voss K, et al.: MTHFD2 is a metabolic checkpoint controlling effector and regulatory T cell fate and function. Immunity 2022;55:65-81.e9.

13. Zhu Z, Leung GKK: More Than a Metabolic Enzyme: MTHFD2 as a Novel Target for Anticancer Therapy? Front Oncol 2020;10:658.

14. Nilsson R, Jain M, Madhusudhan N, et al.: Metabolic enzyme expression highlights a key role for MTHFD2 and the mitochondrial folate pathway in cancer. Nature communications 2014;5:3128.

15. Ju HQ, Lu YX, Chen DL, et al.: Modulation of Redox Homeostasis by Inhibition of MTHFD2 in Colorectal Cancer: Mechanisms and Therapeutic Implications. Journal of the National Cancer Institute 2019;111:584-96.

16. Ron-Harel N, Santos D, Ghergurovich JM, et al.: Mitochondrial Biogenesis and Proteome Remodeling Promote One-Carbon Metabolism for T Cell Activation. Cell metabolism 2016;24:104-17.

17. Sugiura A, Andrejeva G, Voss K, et al.: MTHFD2 is a metabolic checkpoint controlling effector and regulatory T cell fate and function. Immunity 2022;55:65-81 e9.

18. Zhang H, Wu J, Zou D, et al.: Ablation of interferon regulatory factor 4 in T cells induces "memory" of transplant tolerance that is irreversible by immune checkpoint blockade. Am J Transplant 2019;19:884-93.

19. Ogawa M, Suzuki J-i, Hishikari K, Takayama K, Tanaka H, Isobe M: Clarithromycin attenuates acute and chronic rejection via matrix metalloproteinase suppression in murine cardiac transplantation. Journal of the American College of Cardiology 2008;51:1977-85.

20. Freuchet A, Salama A, Bézie S, et al.: IL-34 deficiency impairs FOXP3+ Treg function in a model of autoimmune colitis and decreases immune tolerance homeostasis. Clinical and Translational Medicine 2022;12:e988.

21. Magee CN, Murakami N, Borges TJ, et al.: Notch-1 Inhibition Promotes Immune Regulation in Transplantation Via Regulatory T Cell-Dependent Mechanisms.

Circulation 2019;140:846-63.

22. Hua X, Hu G, Hu Q, et al.: Single-Cell RNA Sequencing to Dissect the Immunological Network of Autoimmune Myocarditis. Circulation 2020;142:384-400.

23. Chen Z, Xu H, Li Y, et al.: Single-Cell RNA sequencing reveals immune cell dynamics and local intercellular communication in acute murine cardiac allograft rejection. Theranostics 2022;12:6242-57.

24. Sugiura A, Andrejeva G, Voss K, et al.: MTHFD2 is a metabolic checkpoint controlling effector and regulatory T cell fate and function. Immunity 2022;55.

25. Pikman Y, Puissant A, Alexe G, et al.: Targeting MTHFD2 in acute myeloid leukemia. J Exp Med 2016;213:1285-306.

26. Sinclair LV, Howden AJ, Brenes A, et al.: Antigen receptor control of methionine metabolism in T cells. Elife 2019;8.

27. Yu W, Wang Z, Zhang K, et al.: One-Carbon Metabolism Supports S-Adenosylmethionine and Histone Methylation to Drive Inflammatory Macrophages. Mol Cell 2019;75:1147-60 e5.

28. Roy DG, Chen J, Mamane V, et al.: Methionine Metabolism Shapes T Helper Cell Responses through Regulation of Epigenetic Reprogramming. Cell metabolism 2020;31:250-66 e9.

29. Brahma S, Henikoff S: CUT&RUN Profiling of the Budding Yeast Epigenome. Methods Mol Biol 2022;2477:129-47.

30. de Candia P, Matarese G: The folate way to T cell fate. Immunity 2022;55:1-3.

31. Lu C, Thompson CB: Metabolic regulation of epigenetics. Cell metabolism 2012;16:9-17.

32. Borges TJ, Murakami N, Lape IT, et al.: Overexpression of PD-1 on T cells promotes tolerance in cardiac transplantation via ICOS-dependent mechanisms. JCI Insight 2021;6.

33. Møller SH, Hsueh PC, Yu YR, Zhang L, Ho PC: Metabolic programs tailor T cell immunity in viral infection, cancer, and aging. Cell metabolism 2022;34:378-95.

34. Yang M, Vousden KH: Serine and one-carbon metabolism in cancer. #N/A 2016;16:650-62.

35. Locasale JW: Serine, glycine and one-carbon units: cancer metabolism in full circle. #N/A 2013;13:572-83.

36. German NJ, Haigis MC: Sirtuins and the Metabolic Hurdles in Cancer. Curr Biol 2015;25:R569-83.

37. Hirschey MD, DeBerardinis RJ, Diehl AME, et al.: Dysregulated metabolism contributes to oncogenesis. Semin Cancer Biol 2015;35 Suppl:S129-s50.

38. Ducker GS, Chen L, Morscher RJ, et al.: Reversal of Cytosolic One-Carbon Flux Compensates for Loss of the Mitochondrial Folate Pathway. Cell Metab 2016;23:1140-53.

39. Morscher RJ, Ducker GS, Li SH, et al.: Mitochondrial translation requires folate-dependent tRNA methylation. Nature 2018;554:128-32.

40. Mentch SJ, Locasale JW: One-carbon metabolism and epigenetics: understanding the specificity. Ann N Y Acad Sci 2016;1363:91-8.

41. Belk JA, Daniel B, Satpathy AT: Epigenetic regulation of T cell exhaustion. Nat Immunol 2022;23:848-60.

42. Man K, Gabriel SS, Liao Y, et al.: Transcription Factor IRF4 Promotes CD8(+) T Cell Exhaustion and Limits the Development of Memory-like T Cells during Chronic Infection. Immunity 2017;47:1129-41 e5.

43. Sun L, Li CW, Chung EM, et al.: Targeting Glycosylated PD-1 Induces Potent Antitumor Immunity. Cancer Res 2020;80:2298-310.

44. Ito T, Naini BV, Markovic D, et al.: Ischemia-reperfusion injury and its relationship with early allograft dysfunction in liver transplant patients. American Journal of Transplantation : Official Journal of the American Society of Transplantation and the American Society of Transplant Surgeons 2021;21:614-25.

45. Dashkevich A, Raissadati A, Syrjälä SO, et al.: Ischemia-Reperfusion Injury Enhances Lymphatic Endothelial VEGFR3 and Rejection in Cardiac Allografts.

American Journal of Transplantation : Official Journal of the American Society of Transplantation and the American Society of Transplant Surgeons 2016;16:1160-72.

46. Pham MX, Teuteberg JJ, Kfoury AG, et al.: Gene-expression profiling for rejection surveillance after cardiac transplantation. The New England journal of medicine 2010;362:1890-900.

Figures and Figure Legends

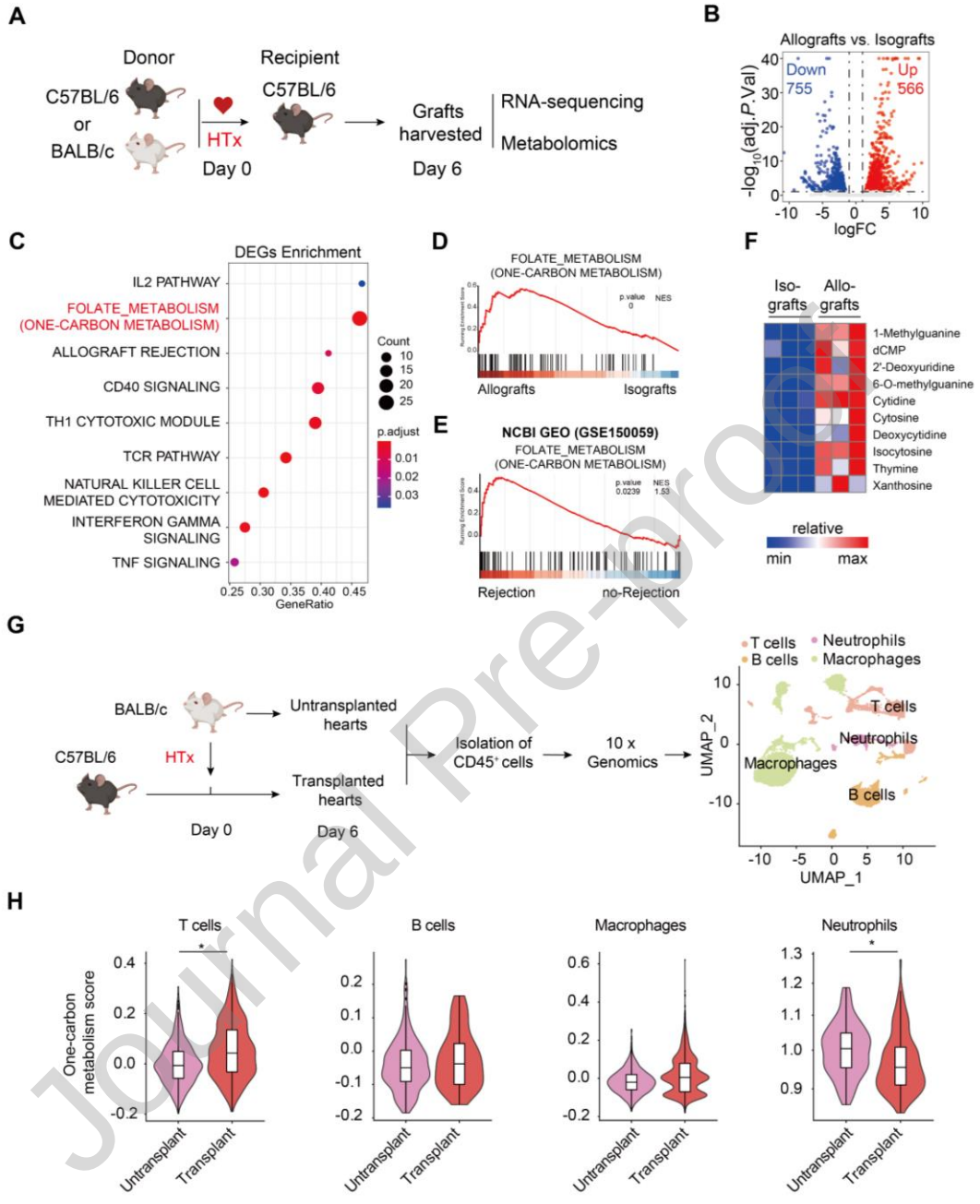

Figure 1. 1C metabolism is differentially active in graft-infiltrating T cells during heart transplant rejection.

(A) Schematic of the RNA-seq and metabolomics analysis workflow. We established murine heterotopic heart transplantation models, including the isograft group (C57BL/6 to C57BL/6) and allograft group (BALB/c to C57BL/6). Grafts were harvested on day 6 after transplantation for RNA-seq and metabolomics assays.

(B) Transcriptome analysis of recipient mouse grafts. Volcano plot of significantly upregulated (red, 566) and downregulated (blue, 755) genes identified by comparing the allografts with isografts.

(C) Dot plot showing the significantly enriched pathways among the DEGs identified between allografts and isografts.

(D) GSEA showing a representative enrichment plot of the folate metabolism (1C metabolism) gene set comparing allografts with isografts.

(E) GSEA showing a representative enrichment plot of the folate metabolism (1C metabolism) gene set comparing endomyocardial biopsies (EMBs) from rejection patients with EMBs from nonrejection patients after heart transplantation. Data were obtained from NCBI GEO (GSE150059).

(F) Heatmap showing the expression levels of 1C metabolism-associated metabolites in allografts and isografts.

(G) Schematic of the workflow used for the scRNA-Seq analysis of $CD45^+$ immune cells in untransplanted and transplanted hearts. UMAP visualization of 4 immune cell types.

(H) Violin plots showing the 1C metabolism enrichment scores of T cells, B cells, macrophages, and neutrophils.

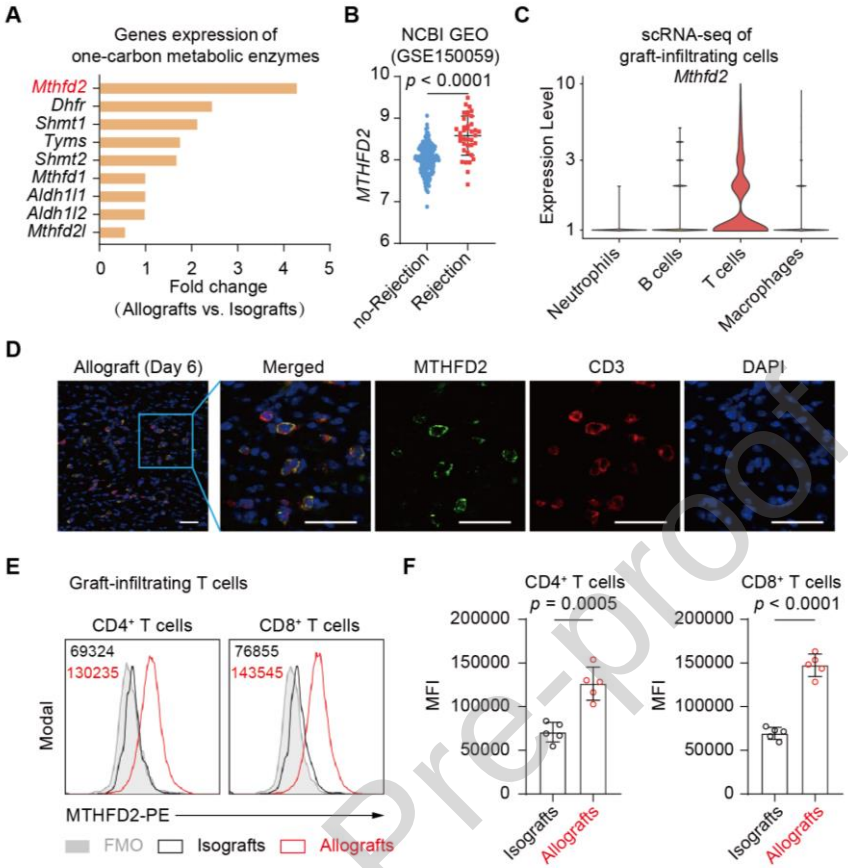

Figure 2. The 1C metabolic enzyme MTHFD2 is expressed at high levels in GITs during heart transplant rejection.

(A, C-F) BALB/c or C57BL/6 (B6) hearts were transplanted into C57BL/6 (B6) mice (n = 5). Grafts were evaluated on day 6 post transplantation.

(A) Histogram showing the fold changes in the expression of genes encoding 1C metabolism enzymes in the comparison of allografts with isografts using RNA-seq.

(B) Bar plots showing the *MTHFD2* expression level in EMBs from rejection patients and EMBs from nonrejection patients after heart transplantation. Data were obtained from NCBI GEO (GSE150059).

(C) Violin plots showing the expression levels of *Mthfd2* among 4 immune cell types in transplanted hearts.

(D) Mouse cardiac allografts were collected on day 6 after transplantation. MTHFD2 and CD3 levels in allografts were detected by performing immunofluorescence staining (MTHFD2, green; CD3, red; DAPI, blue). Scale bars: 50 μm.

(E-F) Representative FCM histograms and bar graphs of the median fluorescence intensity of MTHFD2 in graft-infiltrating $CD4^+$ (left panel) and $CD8^+$ (right panel) T cells. n = 5; two-tailed unpaired Student's t test.

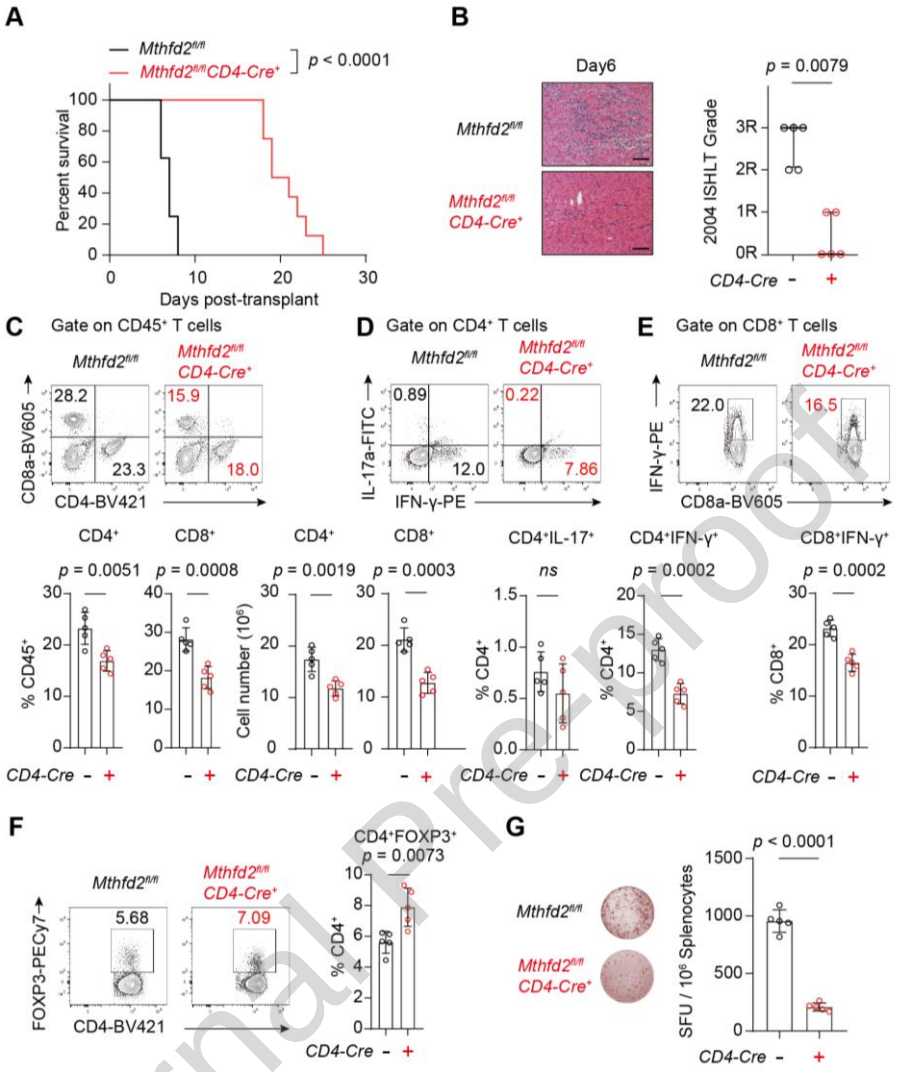

Figure 3. T-cell-specific *Mthfd2* deficiency ameliorates heart transplant rejection in mice.

BALB/c hearts were transplanted into *Mthfd2*$^{fl/fl}$ or *Mthfd2*$^{fl/fl}$*Cd4-Cre*$^{+}$ mice. Grafts and spleens were harvested on day 6 post-transplantation.

(A) The survival curve of cardiac allografts in *Mthfd2*$^{fl/fl}$ and *Mthfd2*$^{fl/fl}$*Cd4-Cre*$^{+}$ recipients. n = 7; log-rank (Mantel Cox) test, $p < 0.0001$.

(B) Representative H&E-stained sections of *Mthfd2*$^{fl/fl}$ and *Mthfd2*$^{fl/fl}$*Cd4-Cre*$^{+}$ allografts collected on day 6 posttransplantation. Scale bars: 100 μm. Data were presented as the interquartile range, n = 5; Mann–Whitney U test, $p = 0.0079$.

(C-F) Splenocytes were isolated from recipient mice and stained with antibodies for FCM.

(C) Representative FCM plots and bar graphs of the percentages and numbers of $CD4^+$, $CD8^+$. n = 5; two-tailed unpaired Student's t test.

(D-F) Representative FCM plots and bar graphs of the percentages of $CD4^+IL\text{-}17^+$, $CD4^+IFN\text{-}\gamma^+$, $CD8^+IFN\text{-}\gamma^+$, and $CD4^+Foxp3^+$ T cells. n = 5; two-tailed unpaired Student's t test.

(G) ELISpot assay of splenic IFN-γ-producing alloreactive cells in mice. n = 5; two-tailed unpaired Student's t test, $p < 0.0001$.

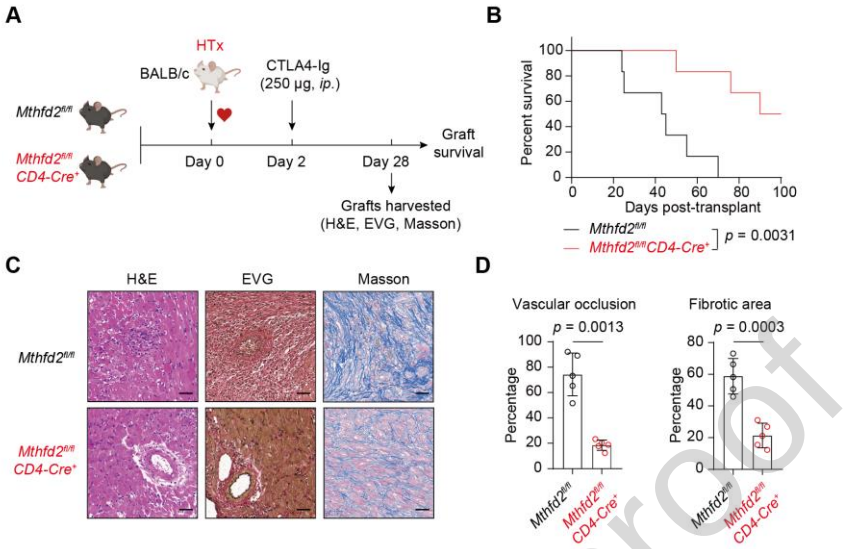

Figure 4. *Mthfd2* deficiency achieves long-term survival in mouse models of chronic cardiac transplant rejection.

Mthfd2$^{fl/fl}$ or *Mthfd2*$^{fl/fl}$*Cd4-Cre*$^{+}$ mice were transplanted with BALB/c hearts on day 0 and were treated with 250 μg CTLA4-Ig on day 2. Grafts were harvested on day 28.

(A) Schematic of the experimental workflow.

(B) The survival curve of cardiac allografts in *Mthfd2*$^{fl/fl}$ and *Mthfd2*$^{fl/fl}$*Cd4-Cre*$^{+}$ mice. n = 6; Log-rank (Mantel-Cox) test, $p = 0.0003$.

(C) Representative H&E, EVG and Masson staining sections of allografts collected on day28 post-transplant. Scale bars: 100 μm.

(D) Bar graphs showing the vascular occlusion of allografts, two-tailed unpaired Welch's t test, $p = 0.0013$ and fibrotic area of allografts, two-tailed unpaired Student's t test, $p = 0.0003$. n = 5.

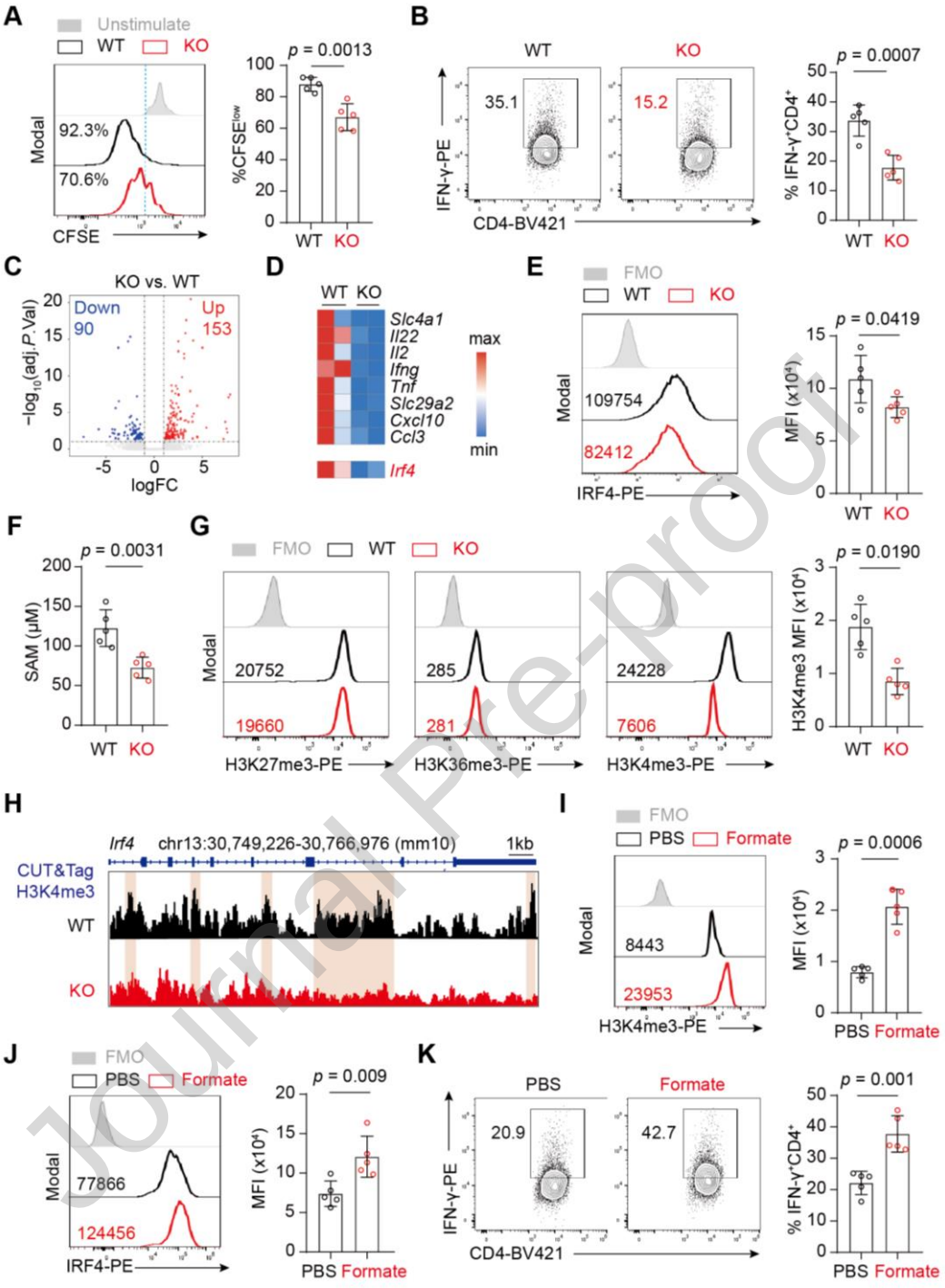

Figure 5. MTHFD2 is required for the function and IRF4 expression of alloreactive T cells in an H3K4me3-dependent manner.

TEa$^{Mthfd2\text{-}KO}$ cells (KO) and TEa^{WT} cells (WT) were labelled with CFSE and cocultured with mitomycin-treated APCs from BALB/c x C57BL/6 F1 mouse spleens at a ratio of 2:1 for 3 days.

(A) Representative FCM histograms and bar graphs of the percentage of $CFSE^{low}$ TEa cells. n = 5; two-tailed unpaired Student's t test, $p = 0.0013$.

(B) Representative FCM plots and bar graphs of the percentage of IFN-γ-positive TEa cells. n = 5; two-tailed unpaired Student's t test, $p = 0.0007$.

(C) Transcriptome analysis of TEa cells following MLR. Volcano plot of significantly upregulated (red, 90) and downregulated (blue, 153) genes identified by comparing KO with WT.

(D) Heatmap showing the representative genes that were changed in the comparison between WT and KO mice.

(E) Representative FCM histograms and bar graphs of IRF4 MFI on TEa cells. n = 5; two-tailed unpaired Student's t test, $p = 0.0419$.

(F) The SAM concentration in the medium following MLR, as measured using ELISA. n = 5; two-tailed unpaired Student's t test, $p = 0.0031$.

(G) Representative FCM histograms (left panel) of H3K27me3, H3K36me3 and H3K4me3 MFIs on TEa cells and bar graphs of the H3K4me3 MFI in TEa cells. n = 5; two-tailed unpaired Welch's t test, $p = 0.0190$.

(H) Representative alignments of CUT&Tag peaks depicting H3K4me3 binding to the *Irf4* loci of WT and KO TEa cells on day 3 following MLR.

(I) Representative FCM histograms and bar graphs of H3K4me3 MFI in TEa cells following MLR with PBS and Formate treatment. n = 5; two-tailed unpaired Welch's t test, $p = 0.0006$.

(J) Representative FCM histograms and bar graphs of IRF4 MFI in TEa cells following MLR with PBS and formate treatment. n = 5; two-tailed unpaired Student's t test, $p = 0.009$.

(K) Representative FCM plots and bar graphs of the percentage of IFN-γ-positive TEa cells following MLR with PBS and formate treatment. n = 5; two-tailed unpaired Student's t test, $p = 0.001$.

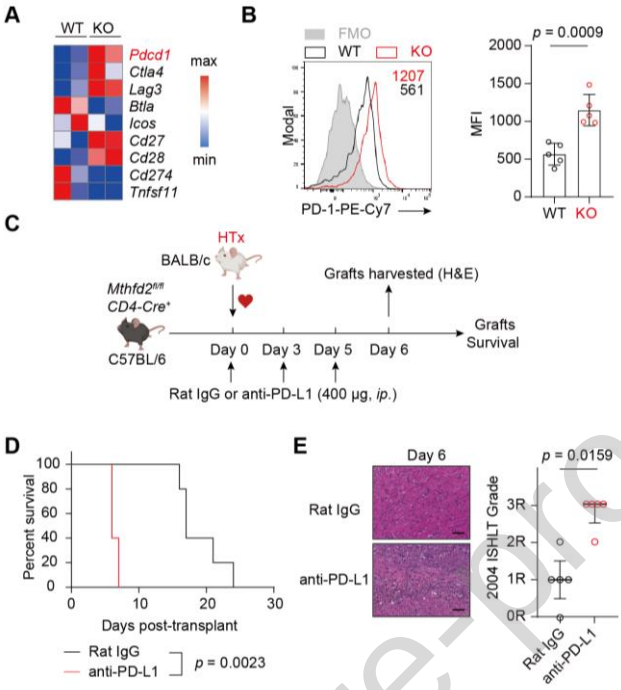

Figure 6. The protective effect of *Mthfd2* ablation on heart transplant rejection depends on the PD-1 pathway.

(A) Heatmap showing the mRNA expression of costimulatory and coinhibitory molecules in WT and *Mthfd2*-deficient TEa cells following MLR.

(B) Representative FCM histograms and bar graphs of PD-1 MFI in WT and *Mthfd2*-deficient TEa cells. n = 5; two-tailed unpaired Student's t test, $p = 0.0009$.

(C) Schematic of the anti-PD-L1 treatment experimental workflow.

(D) The survival curve of cardiac allografts in T-cell-specific *Mthfd2*-deficient mice after treatment with rat IgG and anti-PD-L1 antibodies. n = 5; log-rank (Mantel–Cox) test, $p = 0.0023$.

(E) Representative H&E-stained sections of rat IgG- and anti-PD-L1-treated allografts collected on day 6 posttransplantation. Scale bars: 100 μm. The cellular rejection level was scored according to the 2004 ISHLT guidelines. Data were presented as the interquartile range, n = 5; Mann–Whitney U test, $p = 0.0159$.

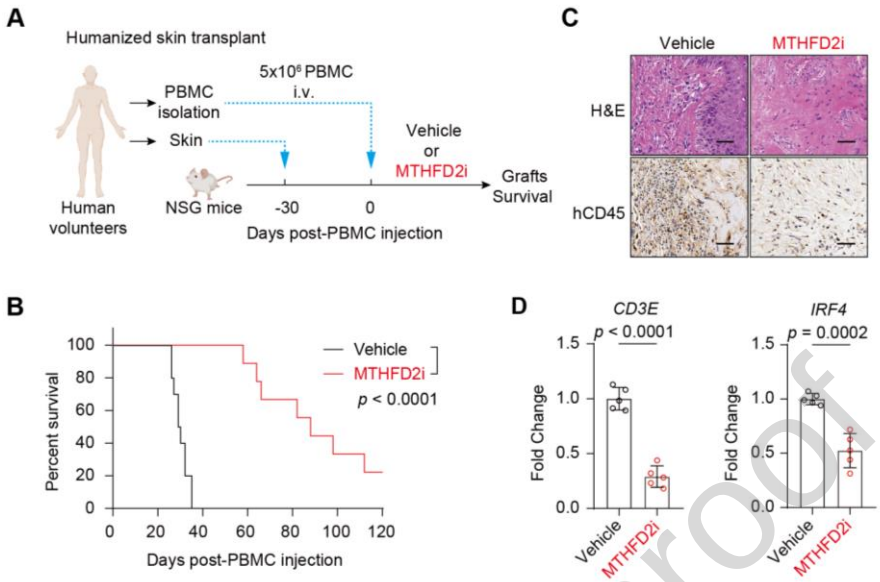

Figure 7. MTHFD2i administration attenuates human allograft rejection in humanized mice.

(A) Schematic of the humanized skin transplant experimental workflow.

(B) The survival curve of human skin allografts in PBMC-injected NSG mice treated with vehicle or MTHFD2i. n = 10; log-rank (Mantel–Cox) test, $p < 0.0001$.

(C) Representative images of H&E and human CD45 IHC staining in vehicle- and MTHFD2i-treated skin allografts collected on day 28 after PBMC injection. Scale bars: 100 μm.

(D) RT–PCR analysis of *CD3E* and *IRF4* mRNA levels in vehicle- and MTHFD2i-treated skin allografts. Plots show the fold change relative to naïve mice. n = 5; two-tailed unpaired Student's t test.

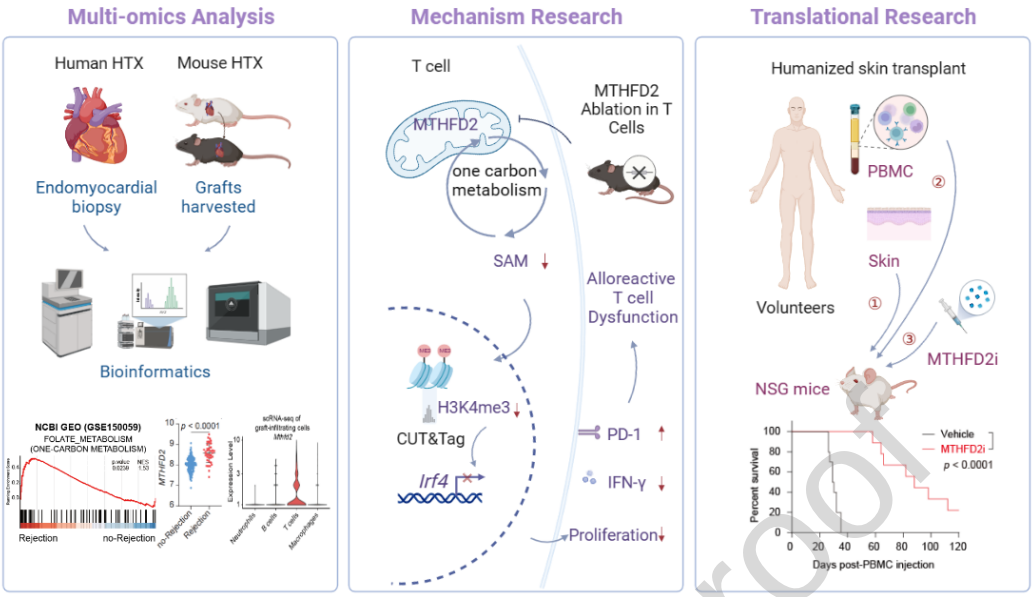

Figure 8. Summary graph of this study.

Multiomics analysis and study of cardiac tissue from human and mouse heart transplant rejection revealed that 1C metabolism is prominently active in cardiac allografts with transplant rejection. *In vitro* assays revealed that MTHFD2 regulated the function and IRF4/PD-1 pathway in T cells through a metabolic-epigenetic mechanism involving SAM and H3K4me3. The humanized skin transplant study revealed that an inhibitor of MTHFD2 attenuated human allograft rejection. The figure was created in Biorender.com.